*Journal of Applied Electrochemistry* **30**: 231–238, 2000.



# Effects of chloride, bromide and iodide ions on internal stress in films deposited during high speed nickel electroplating from a nickel sulfamate bath

Y. TSURU[1], M. NOMURA[1] and F.R. FOULKES[2]
[1]*Department of Materials Science and Engineering, Kyushu Institute of Technology, 1-1, Sensui, Tobata, Kitakyushu, 804, Japan*
[2]*Department of Chemical Engineering and Applied Chemistry, University of Toronto, Toronto, Ontario, M5S 3E5, Canada*

Received 5 June 1998; accepted in revised form 24 August 1999

*Key words:* halide addition, high speed electroplating, internal stress, nickel films, nickel sulfamate bath

**Abstract**

The effects of chloride, bromide and iodide additions on the internal stress developed in nickel films deposited during high speed electroplating from nickel sulfamate baths operated close to the nickel ion limiting current density were investigated. The variations in internal strain in the films were detected *in situ* using a resistance wire-type strain gauge placed on the reverse side of the copper substrate. The film resistance on the as-plated electrodes was measured using an electronic current interrupter technique. The effects of chloride, bromide, and iodide additions could be classified into two groups: (a) chloride and bromide ions, and (b) iodide ions. For chloride and bromide additions over the concentration range of 0.1 to 0.5 M, the nickel deposits exhibited a block- and pyramid-like texture with a (2 0 0) crystal orientation. The internal tensile stress developed in 20 $\mu$m thick nickel films deposited in the presence of these two halides was as low as 140–170 MPa. Conversely, for additions of iodide, at iodide concentrations greater than 0.1 M the deposited nickel exhibited a fine granular texture of disordered crystal orientation. The internal tensile stress developed in 20 $\mu$m thick nickel films deposited from these latter baths tended to rise with increasing iodide concentration to values considerably higher than those observed at similar concentrations of $NiCl_2$ or $NiBr_2$.

## 1. Introduction

High speed electroplating recently has become widely used in the industrial mass production of components used in electronic instruments. High speed nickel electroplating, in particular, has become popular as a microelectroforming technique for the manufacture of microsystem technologies [1, 2]. For such applications, nickel sulfamate baths containing boric acid additions are favored over standard Watts-type baths because the nickel films obtained from a sulfamate bath (especially thick films) typically have lower tensile stresses than films of similar thickness obtained from a Watts bath [3]. The anodes used with such baths typically consist of nickel, to which has been added low (e.g., 0.02 wt %) amounts of sulfur to promote dissolution [4, 5]. However, nickel anodes tend to form resistive passive films on their surfaces [6], and the highly positive anodic potentials generally associated with high speed nickel electroplating tend to increase this passivity, resulting in increased applied cell voltage, increased power costs, unwanted changes in the pH and nickel ion concentration of the bath, and even in decomposition of sulfamate ion [7, 8].

To alleviate these problems, halide ions usually are added to the plating bath to promote the dissolution of the anode by destabilizing the passive film on its surface. However, chloride or iodide ions tend to raise the tensile stress in the deposited nickel films [9]; conversely, bromide ions at the same concentration tend somewhat to decrease it [10]. Thus, any discussion of the effects of halide ion additions must take into account not only the reduction of anode passivity, but also the tensile stress in the electrodeposited films that are produced.

In this paper we report on our studies of the effects of chloride, bromide and iodide ion additions on the internal tensile stress in films produced during high speed nickel electroplating from sulfamate baths operated close to the nickel ion limiting current density.

## 2. Experimental details

The compositions of the sulfamate baths employed are given in Table 1. Each halide was added to the bath as $NiX_2$ (where X = $Cl^-$, $Br^-$ or $I^-$) with the total concentration of nickel ions in each bath kept constant at 1.55 M. Each bath also contained 0.81 M boric acid,

*Table 1.* Composition of nickel sulfamate baths used for high speed electroplating

| Bath | A | B | C | D | E | F | G |
|---|---|---|---|---|---|---|---|
| $Ni(OSO_2NH_2)_2$/M | 1.55 | 1.54 | 1.53 | 1.50 | 1.45 | 1.35 | 1.05 |
| $NiX_2^*$/M | – | 0.01 | 0.02 | 0.05 | 0.10 | 0.20 | 0.50 |
| $H_3BO_3$/M | 0.81 | 0.81 | 0.81 | 0.81 | 0.81 | 0.81 | 0.81 |
| pH | 4.0 | 4.0 | 4.0 | 4.0 | 4.0 | 4.0 | 4.0 |

* $X = Cl^-$, $Br^-$, $I^-$

which has been shown to inhibit hydrogen evolution during the nickel electrodeposition process at high current densities close to the nickel ion limiting current density, and, consequently, to suppress any increases in the internal stress in the deposited nickel film [11, 12]. In order to avoid any effects of concomitant oxidation of the sulfamate ion, the surface area of the 99.99% pure nickel foil counter electrode was made relatively large (10 $cm^2$); also, for each experiment the 150 mL of electrolyte was replenished after the passage of 120 C of electricity, corresponding to a deposited nickel film thickness of approximately 20 $\mu$m. The electroplating was carried out galvanostatically at 50 °C in a beaker-type cell without stirring at a current density of 18.0 A $dm^{-2}$, corresponding to approximately 90% of the nickel ion limiting current density. For each experiment the substrate metal receiving the deposit consisted of a 25 mm × 8 mm rectangular piece of 0.6 mm thick commercial copper foil (99.9% Cu). After cutting, each copper electrode was annealed in a vacuum at 350 °C for 2 h, followed by electropolishing at room temperature for about 5 min in 50 vol % phosphoric acid before use. As mentioned above, the counter electrode consisted of a piece of commercial nickel foil of 99.99% purity. All potentials were measured and reported against the Ag/AgCl sat. KCl reference electrode (0.197 V vs SHE at 25 °C).

The average internal strains in the deposited nickel films were determined *in situ* using a resistance wire-type strain gauge fixed to the reverse side of the copper substrate [13]. This strain gauge, which expands and contracts with the bending of the copper substrate during the electroplating process, has been shown to precisely reflect the residual stress in the nickel deposit [14]. The internal stresses in the deposits were calculated from the internal strains using values of Young's modulus and Poisson's ratio of, respectively, 201.0 GPa and 0.31 for the nickel film, and 122.6 GPa and 0.34, respectively, for the copper substrate [15]. The values of internal stress obtained using this method are similar to those that would be obtained using the spiral contractometer method [16]. A Hokuto Denko (model HC-110) current interrupter set at a pulse time of 50 ms and a duty cycle of 50% was used to measure the *IR*-drop [17], which consisted of the film resistance of the as-plated electrode and the solution resistance between the electrode and the tip of the Luggin capillary, the latter being maintained at a distance of 2 mm from the surface of the depositing film. The specific conductivities of the plating baths were measured using a Hitachi-Horiba (model DS-12) conductivity meter. The amounts of deposited nickel were determined by dissolving the nickel films in acid and using an atomic absorption analyser to measure the nickel concentrations of the resulting solutions. X-ray diffraction (XRD) and scanning electron microscopy (SEM) were used to determine the crystal structure and the morphology, respectively, of the nickel deposits.

## 3. Results and discussion

### 3.1. *Effects of halide ions on internal stress of deposit*

Figure 1 shows the internal tensile stress in nickel films plated at 18.0 A $dm^{-2}$ as a function of film thickness for different concentrations of chloride ion added to the bath. Similar plots for additions of bromide ion and iodide ion are presented in Figures 2 and 3, respectively. Although the behaviour at times is a complex function of halide ion concentration, in general, Figures 1 to 3 indicate that the internal tensile stress in the plated films increased in the order of $NiCl_2 < NiBr_2 < NiI_2$. Near the beginning of the electroplating (i.e., for 1.0 $\mu$m thick films) the internal tensile stresses in the nickel films plated from baths containing chloride ions and bromide ions were more or less in excess of 400 MPa; as the plating proceeded and the films thickened, the stresses gradually fell to lower values. However, from Figure 3 it

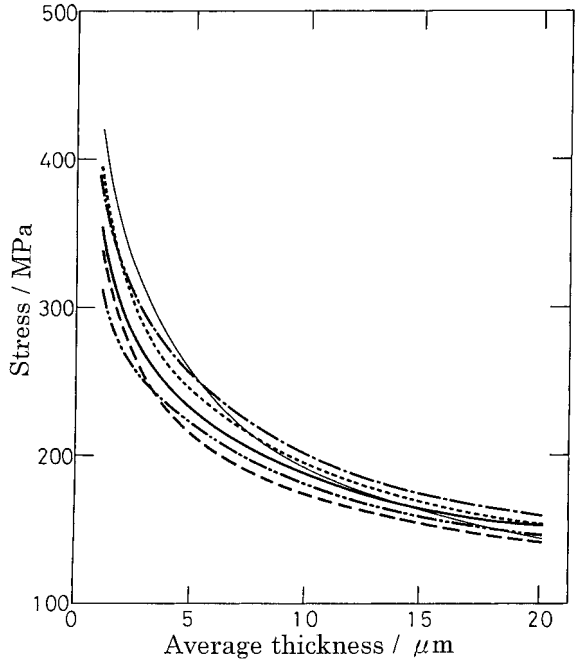


*Fig. 1.* Typical example of relation between internal tensile stress and average film thickness for nickel films electrodeposited at 50 °C from sulfamate baths containing different amounts of $NiCl_2$. [$NiCl_2$]: (——) 0, (▬▬) 0.02, (- - - - -) 0.05, (– – –) 0.10, (– – – –) 0.20 and (– – – – –) 0.50 M.

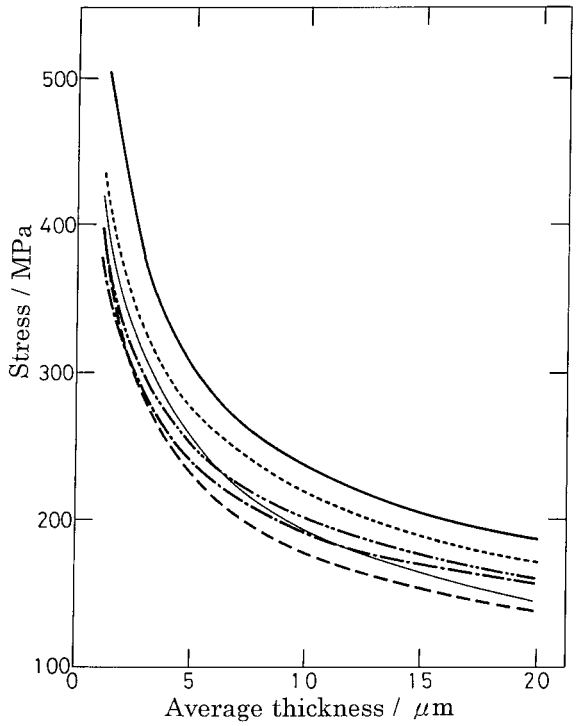


*Fig. 2.* Typical example of relation between internal tensile stress and average film thickness for nickel films electrodeposited at 50 °C from sulfamate baths containing different amounts of $NiBr_2$. [$NiBr_2$]: (——) 0, (▬▬) 0.02, (- - - - -) 0.05, (– – –) 0.10, (– – – –) 0.20 and (– - – - – -) 0.50 M.

can be seen that the initial behaviour (1.0 $\mu$m thick films) was more complex in the case of iodide ion additions: at low concentrations the stress was initially high, but decreased as the concentration of $NiI_2$ increased, passing through a minimum around 0.05 M $NiI_2$, after which it gradually increased again with increasing iodide concentration.

Hoar and Arrowsmith [18] explained qualitatively the origin of these observed tensile stresses on the basis of dislocation theory, according to which the strains develop because of the misfit between the nickel deposit and the copper substrate when the former continues the structure of the latter. The stresses which can develop when such epitaxial deposition occurs can be very high [19, 20]. In the present study, calculations indicate that the percentage of misfit was 2.6% for the Ni [1 0 0] // Cu [1 0 0] axis in the Ni (1 0 0) // Cu (1 0 0) planes [21].

Returning to the effect of the iodide ion, it is noted from Figure 3 that for $NiI_2$ additions at concentrations greater than 0.02 M, the internal tensile stress passed through a maximum with increasing film thickness, and then gradually decreased. Figure 4 shows that, in general, the higher the iodide concentration, the greater was this maximum value of the tensile stress, and the thinner was the film thickness at the maximum value. On account of the formation of cuprous iodide, which is a slightly soluble salt ($K_{SP} = 5.1 \times 10^{-12}$ at 20 °C), iodide ions tend to adsorb on the copper substrate more strongly than chloride and bromide ions [22, 23]. Consequently, it would appear that these adsorbed iodide ions are able to interfere with the epitaxial deposition of nickel onto the copper, resulting in the high stresses observed during the initial stages of the electrodeposition process.

Figure 5 shows the relation between the level of halide ion addition and the resulting internal tensile stress in 20 $\mu$m thick nickel films. Each curve in Figure 5 was obtained by averaging the data from three replicate stress-deposit thickness curves similar to the representative curves shown in Figures 1, 2 and 3. With increasing concentration of each type of halide ion,

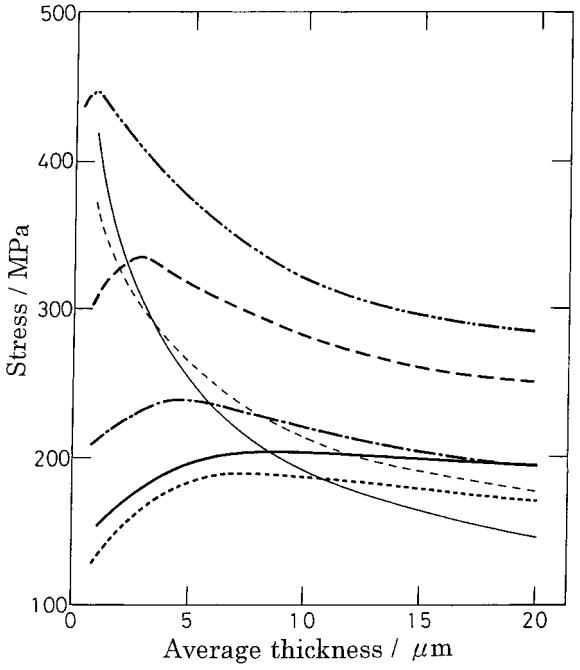


*Fig. 3.* Typical example of relation between internal tensile stress and average film thickness for nickel films electrodeposited at 50 °C from sulfamate baths containing different amounts of $NiI_2$. [$NiI_2$]: (——) 0, (– – – –) 0.01, (▬▬) 0.02, (- - - -) 0.05, (– – –) 0.10, (- - - -) 0.20 and (– - – - – -) 0.50 M.

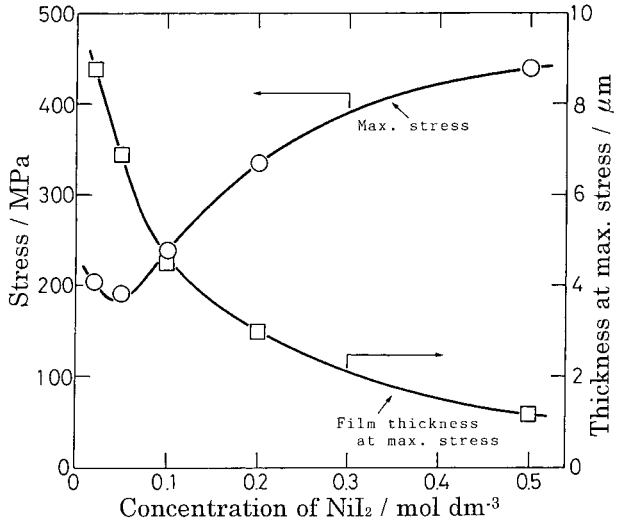


*Fig. 4.* Effect of $NiI_2$ concentration on maximum tensile stress and film thickness at maximum tensile stress.

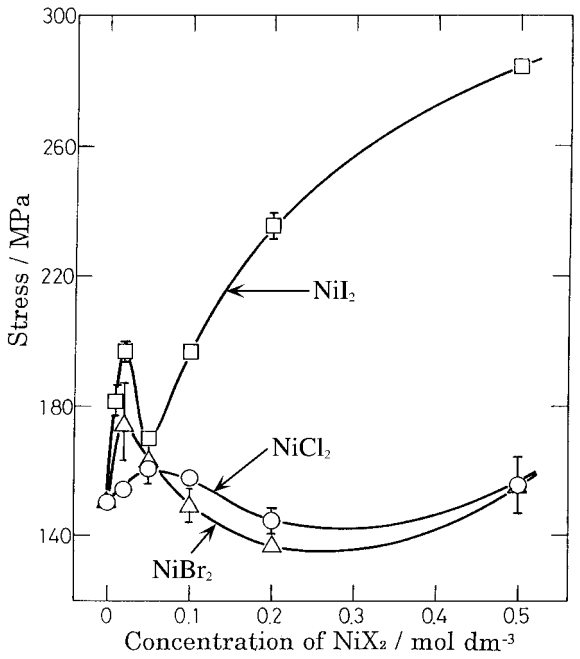


*Fig. 5.* Relation between internal tensile stress in 20 $\mu$m thick nickel films and halide concentration for different halides. Error bars indicate maximum and minimum measured values.

there is an initial increase in the internal tensile stress to a maximum value, followed by a decrease to a minimum value and then a further increase. For $NiI_2$ and $NiBr_2$ additions, the initial maximum value of the tensile stress occurred at a halide concentration of about 0.02 M; for $NiCl_2$ the maximum was at about 0.05 M. Similarly, for $NiI_2$ the corresponding minimum value was observed at about 0.05 M, while for both $NiBr_2$ and $NiCl_2$ the minimum occurred at about 0.25 M. In particular it is noted that at halide additions greater than about 0.1 M, the stresses developed in the presence of iodide ions were much higher than those developed in the presence of bromide ions or chloride ions.

The above results indicate that, in the presence of halide ions, the development of tensile stresses in plated nickel films can occur via more than one mechanism, depending on the concentration of $NiX_2$. For the sulfamate bath used in the present study, the critical concentration of $NiCl_2$, $NiBr_2$ and $NiI_2$ at which the mechanism changes was about 0.1 M. Marti [9], who also studied the effects of halide additions to sulfamate baths – but only in the higher concentration region 0.1–0.5 M – also observed that the stresses developed in the presence of $NiBr_2$ were somewhat lower than those developed in the presence of $NiCl_2$ and much lower than those developed in the presence of $NiI_2$. Thus, although there is general agreement among investigators that the addition of chloride ions raises the stress in the nickel films plated from *Watts*-type baths [24], Figure 5 shows that in the case of *sulfamate* baths operated at high current densities near the limiting current density, $NiCl_2$ additions in the concentration region 0.1–0.5 M do not always result in highly stressed deposited films.

### 3.2. *Surface morphology and crystal structure*

In general, a bath additive affects the surface morphology and crystal structure of an electroplated film. Figure 6 shows the effects of the various halide ions on the surface morphologies and crystal structures of the nickel films plated from the sulfamate baths used in this study. The films plated from baths containing $NiCl_2$ or $NiBr_2$ always consisted of silver–white coloured block- and pyramid-like deposits, which were similar to those obtained from sulfamate bath *A*, containing no halide additions. On the other hand, the surface morphology of the nickel films plated from sulfamate baths containing $NiI_2$ changed from a block- and pyramid-like texture at $NiI_2$ concentrations less than 0.01 M to a fine, granular deposit at $NiI_2$ concentrations greater than 0.02 M; the deposit appearance concomitantly changed from silver-white to dark gray at $NiI_2$ concentrations greater than 0.02 M. These changes in the surface morphology of the deposit with $NiI_2$ concentration correlate very well with the changes in the internal stress in the film, shown in Figure 5. Fine granular deposits such as these are typical of deposits produced during electroplating from baths containing strongly adsorbed additives under conditions exceeding the limiting current density [25].

Figure 7 shows the XRD patterns of the plated nickel films obtained from sulfamate baths containing the various halide ions. The films plated from baths containing $NiCl_2$ or $NiBr_2$ always consisted of nickel with a (2 0 0) crystal orientation; these films were similar to those obtained from sulfamate bath A (no halide additions), and tended to have relatively low tensile stresses. But, as Figure 7 clearly shows, the crystal orientation of the nickel films plated from sulfamate baths containing $NiI_2$ additions was quite different: at low $NiI_2$ concentrations (0.02 M $NiI_2$) the deposits had a (2 0 0) crystal orientation; however, as the $NiI_2$ concentration increased, in addition to nickel having a (2 0 0) crystal orientation, increasing amounts of nickel having a (1 1 1) and a (2 2 0) crystal orientation also started to appear. For the purpose of comparison, the relative intensities of the (1 1 1), (2 0 0) and (2 2 0) planes in ASTM standard nickel powder are 100, 42 and 21, respectively [21]. Therefore, it can be seen that as the $NiI_2$ concentration in the sulfamate bath is increased, the crystal structure of the nickel deposit changes gradually from a (2 0 0) preferred orientation to a disordered orientation that approaches that of standard nickel powder. These results correspond to a change in surface morphology from a block- and pyramid-like texture to a fine granular texture with an increase in the $NiI_2$ concentration.

### 3.3. *Current efficiency*

At a plating current density of 18.0 A $dm^{-2}$, the current efficiency obtained from bath A without any halide ion additions was almost 100%. In general, the addition of a

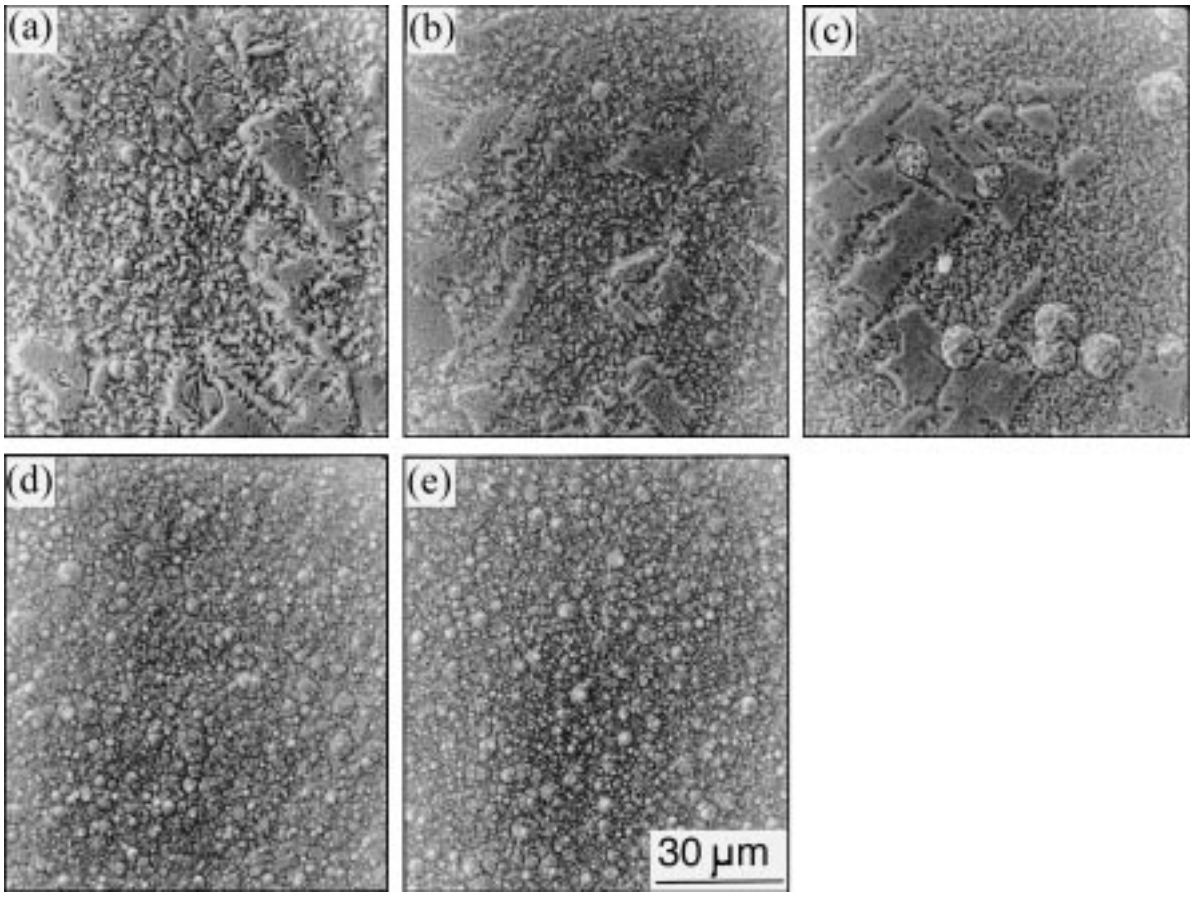


*Fig. 6.* Surface morphology of nickel films obtained from sulfamate baths containing various halide ions. (a) 0.5 M $NiCl_2$, (b) 0.5 M $NiBr_2$, (c) 0.01 M $NiI_2$, (d) 0.02 M $NiI_2$ and (e) 0.5 M $NiI_2$.

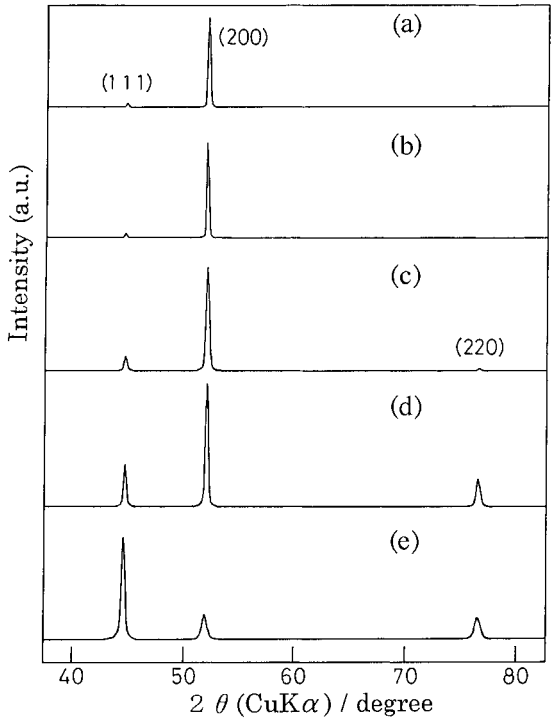


*Fig. 7.* X-ray diffraction patterns of nickel films obtained from sulfamate baths containing various halide ions. (a) 0.5 M $NiCl_2$, (b) 0.5 M $NiBr_2$, (c) 0.02 M $NiI_2$, (d) 0.05 M $NiI_2$ and (e) 0.5 M $NiI_2$.

brightener tends to increase the cathodic overpotential for the electrodeposition process, and, consequently, to decrease the current efficiency. The effects of the various halides on the current efficiency are shown in Figure 8. With the addition of halide ions, the current efficiency slightly decreased from 100%, passing through a minimum value of 96% at 0.05 M $NiCl_2$ and of 95% at 0.02 M $NiI_2$. No minimum was observed for the addition of $NiBr_2$. The concentrations of $NiCl_2$ and $NiI_2$ at which the minimum current efficiencies were observed correlate exactly with the maximum values of the internal stresses in the films (see Figure 5). Therefore, hydrogen evolution would seem to enhance the development of tensile stresses in the deposited films when $NiCl_2$ and $NiI_2$ are added at concentrations of less than about 0.05 M [26]. However, this increase in tensile stress is not observed for similar concentrations of $NiBr_2$. As indicated in Figure 5, in the concentration range from 0.05 to 0.5 M, for $NiBr_2$ the internal stress decreased to a minimum of 137 MPa, while for $NiI_2$ it significantly rose from 177 to 284 MPa, despite the fact that the current efficiencies were constant at about 96% for both halides. These results indicate that the observed stresses in the deposited nickel films cannot be explained solely on the basis of hydrogen evolution; other factors also must be at work. For example, it is possible that the

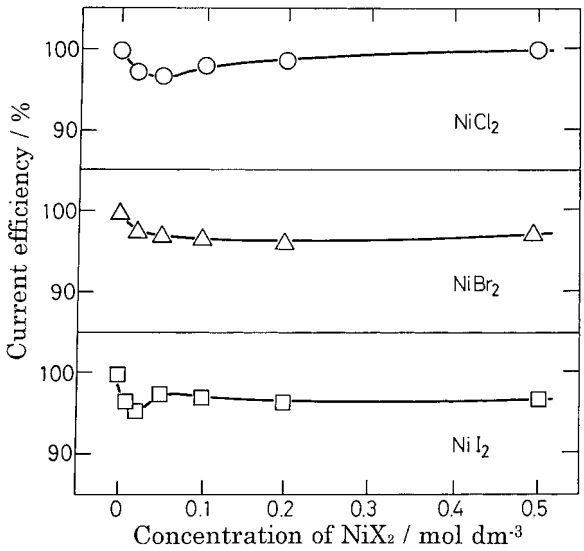


*Fig. 8.* Effect of halide additions on current efficiency of sulfamate baths at 50 °C.

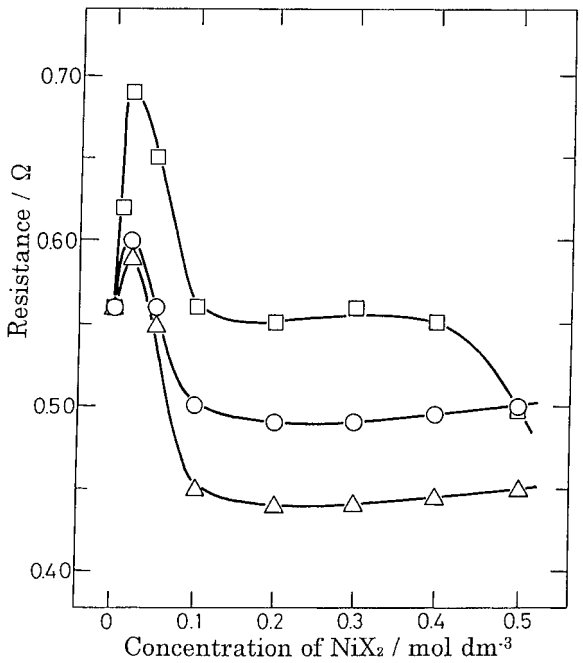


*Fig. 9.* Effect of halide ion concentration on electrical resistance in vicinity of cathode. Key: (○) $NiCl_2$, (△) $NiBr_2$ and (□) $NiI_2$.

increase in solution pH close to the electrode as a consequence of hydrogen evolution may promote the codeposition of $OH^-$ and/or O as hydrated basic Ni salts, $Ni(OH)_2$ or NiO inclusions in the deposits [3]; furthermore, these intermediate species might adsorb halide ions.

### 3.4. *Conductivity of the bath and resistance of electrode film*

When the ratio of the concentration of halide ions in solution to that of $OH^-$ ions in solution exceeds a certain critical value (the exact value depends on the specific conditions), halide ions are able to displace hydroxyl ions from the passive film on the nickel surface, leading to a breakdown of the protective film [27]. Under the steady state plating conditions of the present study, the cathode potentials were −0.955, −0.960 and −1.13 V for plating baths containing 0.02 M $NiCl_2$, 0.02 M $NiBr_2$ and 0.02 M $NiI_2$, respectively. Since the potential of zero charge for nickel is in the order of −0.5 to −0.6 V [28], it would seem that the electrode potentials were too negative for halide ions to readily adsorb onto the electrode surface during the plating process.

Figure 9 shows the effect of the halide ion concentration on the electrical resistance, $R$, obtained from $IR$-drop data measured using the electronic current interrupter procedure described earlier. This electrical resistance consists of the sum of the solution resistance between the tip of the Luggin capillary and the cathode surface plus the resistance of the nickel film on the surface of the cathode. For each type of halide ion, the resistance initially increased to a maximum value at a halide concentration of about 0.02 M, followed by a sudden decrease. For plating baths containing 0.2 M $NiX_2$, the resistance varied in the order $R(I^-) > R(Cl^-) > R(Br^-)$. Over the $NiX_2$ concentration range 0.1–0.5 M the resistance was almost constant for $NiCl_2$ and $NiBr_2$, whereas for $NiI_2$ it was almost constant in the range 0.1–0.4 M and decreased to a lower value in 0.5 M $NiI_2$. Since iodide ions are more easily oxidized than chloride or bromide ions, this decrease in $R$ at the relatively high concentration 0.5 M $NiI_2$ might indicate a decrease in the film resistance as a result of adsorption on the cathode of $I_2$ (or $I_3^-$) produced by the oxidation at the anode of iodide ion to iodine.

From Figure 10, which shows the effect of halide ion concentration on the specific conductivities of the sulfamate plating baths at 50 °C, it is clear that for

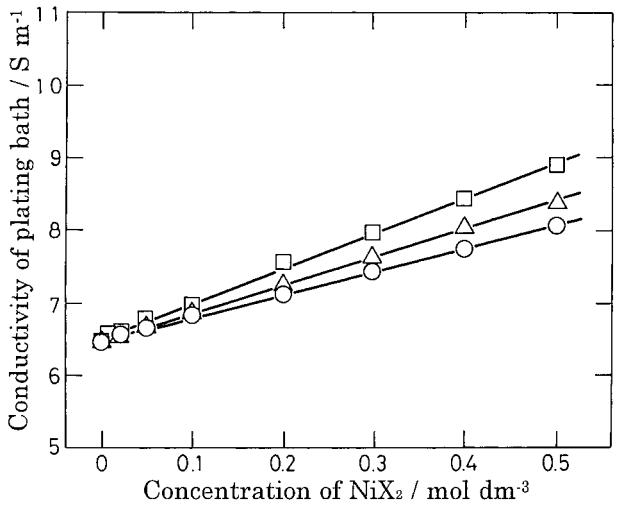


*Fig. 10.* Effect of halide ion concentration on conductivity of sulfamate plating bath at 50 °C. Key: (○) $NiCl_2$, (△) $NiBr_2$ and (□) $NiI_2$.

each type of halide the bath conductivity increases linearly with increasing halide concentration, and that the order of increasing halide conductivity is $NiI_2 > NiBr_2 > NiCl_2$. The regularity of these conductivity data suggests that the unusual variations observed in the resistance data shown in Figure 9 can be attributed to variations in the resistance of the nickel film, rather than to variations in the solution resistance. Furthermore, the striking similarity between the shapes of the stress curves in Figure 5 and the resistance curves in Figure 9 indicates that the stress which develops in a nickel film during the plating process is related to some kind of resistive film which forms on the metal surface [29]. This is further evidence that halide ions almost certainly adsorb on the electrode during electroplating.

Using a chemical impedance procedure, Epelboin and Wiart [30] showed that for Watts baths the following reaction mechanism involving an intermediate species $(NiOH)_{ads}$ plays an important role in the rate-determining step:

$$Ni^{2+} + H_2O \rightleftharpoons NiOH^+ + H^+ \quad (1)$$

$$NiOH^+ + e^- \xrightarrow{RDS} (NiOH)_{ads} \quad (2)$$

$$(NiOH)_{ads} + H^+ \rightleftharpoons Ni + H_2O \quad (3)$$

The observations that for both Watts-type baths and sulfamate baths the same tafel slope of $-0.12$ V $(decade)^{-1}$ is obtained, and that the *IR*-free potential–current density curves for nickel deposition are very similar in each type of bath [31], indicate that an adsorbed nickel hydroxide species such as $(NiOH)_{ads}$ might be formed as a surface intermediate during electroplating from nickel sulfamate baths.

The above reaction mechanism suggests an explanation for the behaviour observed in Figure 9 in the $NiX_2$ concentration region below 0.05 M: In this concentration domain there may be an electrostatic interaction involving the formation of an ion pair in solution:

$$NiOH^+ + X^- \rightleftharpoons NiOH^+X^- \quad (4)$$

Because this ion pair is electrically neutral, it could readily adsorb on the negatively-charged electrode surface, thereby incorporating into the nickel film a hydroxide species which, because of its halide content, would be expected to have a higher electrical resistance than the species $(NiOH)_{ads}$, which is formed in the absence of halides. The greater the halide ion concentration in the bath, the greater will be the concentration of the neutral complex formed, and therefore the greater will be the amount of this complex that will be incorporated into the nickel film. Thus, as shown in Figures 5 and 9, both the internal tensile stress and the film resistance increased with halide concentration, the order being $I^- > Cl^- > Br^-$.

On the other hand, Figure 9 shows that in the $NiX_2$ concentration region greater than 0.1 M a different type of behaviour takes place. At $NiX_2$ concentrations greater than 0.1 M, Philip et al. [32] have reported that the following reaction mechanism takes place simultaneously with Epelboin's mechanism:

$$Ni^{2+} + Cl^- \rightleftharpoons NiCl^+ \quad (5)$$

$$NiCl^+ + e^- \xrightarrow{\text{RDS at low } \eta} (NiCl)_{ads} \quad (6)$$

$$(NiCl)_{ads} + e^- \xrightarrow{\text{RDS at high } \eta} Ni + Cl^- \quad (7)$$

Thus, we can speculate that in the halide concentration region greater than 0.1 M, instead of the formation of $(NiOH)_{ads}$ or $(NiOHX)_{ads}$, some other intermediate species such as $(NiX)_{ads}$ forms on the electrode surface [33]. In the case of $NiCl_2$ and $NiBr_2$ additions, the respective species $(NiCl)_{ads}$ and $(NiBr)_{ads}$ lower both the resistance and the internal tensile stress in the film. Conversely, in the case of $NiI_2$ additions, as the $NiI_2$ concentration increases beyond 0.1 M, the adsorption onto the electrode of $I_3^-$ and/or $I_2$ raises the internal stress in the film and changes the surface morphology from a block- and pyramid-like deposit to a granular deposit.

## 4. Summary

During the high speed electrodeposition of nickel from nickel sulfamate baths at a current density of 18.0 A $dm^{-2}$, the effects of chloride, bromide, and iodide additions on the internal stresses in the plated nickel films can be classified into two groups, the first consisting of chloride and bromide ions, and the second consisting of iodide ions. With increasing halide ion concentration, for all three halides the internal tensile stress in 20 $\mu$m thick deposited nickel films first rose to a maximum value, then decreased to a minimum value, and then started to increase again. In the case of chloride and bromide additions over the concentration range 0.1–0.5 M, the deposited nickel had a silver–white appearance and a block- and pyramid-like texture with a (2 0 0) crystal orientation. The internal tensile stresses developed in 20 $\mu$m thick nickel films deposited in the presence of these two halides were as low as 140–170 MPa. Conversely, for additions of iodide, at concentrations greater than 0.1 M, the deposited nickel exhibited a fine granular texture of disordered crystal orientation, and the deposit appearance changed from silver–white to dark gray at iodide concentrations greater than 0.02 M. The internal tensile stresses developed in 20 $\mu$m thick films deposited from these latter baths at iodide concentrations greater than 0.1 M tended to rise with increasing iodide concentration to values considerably higher than those observed at similar concentrations of $NiCl_2$ or $NiBr_2$.

## References


1. W. Ehrfeld, *in* H. Reichl (Ed.), Proceedings of 1st International Conference on 'Micro Electro, Opto, Mechanical Systems and Components', 'Micro System Technologies 90', (Springer, Berlin, Sept. 1990), pp. 261–2.
2. T. Hirano, T. Furuhata and H. Fujita, *in* Proceedings of IEEE Micro Electro Mechanical Systems Workshop, Fort Lauderdale, FL (Feb. 1993), pp. 278–83.
3. W.H. Safranek, 'The Properties of Electrodeposited Metals and Alloys', 2nd edn, American Electroplaters and Surface Finishing Society, USA (1986), pp. 295–315.
4. G.A. Di Bari and J.V. Petrocelli, *J. Electrochem. Soc.* **112** (1965) 99.
5. I.J. Bear, R.C. Flann, K.J. McDonald, L.J. Rogers and R. Woods, *J. Appl. Electrochem.* **22** (1992) 8.
6. M. Pourbaix, 'Atlas of Electrochemical Equilibria in Aqueous Solutions', 2nd edn, National Association of Corrosion Engineers, USA (1974), pp. 330–42.
7. T. Iwagaki, *Plat. Surf. Finish.* **67** (July 1980) 51.
8. R.J. Kendrick and S.A. Watson, *Electrochim. Metallorum* **1** (1996) 320.
9. J.L. Marti, *Plating* **53** (1966) 61.
10. H. Searles, *Plating* **53** (1966) 204.
11. J. Horkans, *J. Electrochem. Soc.* **126** (1979) 1861.
12. D.A. Fanner and R.A.F. Hammond, *Trans. Inst. Metal Finish.* **36** (1958/9) 32.
13. Y. Tsuru, T. Tamai and K. Hosokawa, *in* Proceedings of 14th World Congress on Interfinish, 'Interfinish 96', Birmingham, UK (Sept. 1996), Vol. 2, pp. 89–99.
14. Y. Tsuru and M. Tanaka, *Denki Kagaku* **64** (1996) 112.
15. H.M. Ledbetter, *Mater. Sci. Engi.* **27** (1977) 133.
16. S. Konishi, *J. Met. Finish. Soc. Japan* **11** (1960) 273.
17. K.R. Williams, 'Introduction to Fuel Cells', (Elsevier, New York, 1966), pp. 57–63.
18. T.P. Hoar and D.J. Arrowsmith, *Trans. Inst. Metal Finish.* **36** (1958/9) 1.
19. C. Marie and J. Thon, *Compt. Rend.* **193** (1931) 31.
20. H. Watkins and A. Kolk, *J. Electrochem. Soc.* **108** (1961) 1018.
21. ASTM, 'X-ray powder data file', Sets 1–5, 4-0836, 4-0850 (ASTM, Philadelphia, PA, 1960).
22. D. Jope, J. Sell, H.W. Pickering and K.G. Weil, *J. Electrochem. Soc.* **142** (1995) 2170.
23. H. Uchida, N. Ikeda and M. Watanabe, *J. Electroanal. Chem.* **424** (1997) 5.
24. A. Brenner, V. Zentner and C.W. Jennings, *Plating* **39** (1952) 865.
25. J. O'M. Bockris and M. Enyo, *Trans. Faraday Soc.* **58** (1962) 1187.
26. A. Knödler, *Metallöberflache* **20** (1966) 52.
27. U.R. Evans, *J. Chem. Soc., Lond.* (1930) 1773.
28. J. O'M. Bockris, S.D. Argade and E. Gileadi, *Electrochim. Acta* **14** (1969) 1267.
29. F. Zucchi, M. Fonsati and G. Trabanelli, *J. Appl. Electrochem.* **28** (1998) 441.
30. I. Epelboin and R. Wiart, *J. Electrochem. Soc.* **118** (1971) 1577.
31. Y. Tsuru, M. Nomura and F.R. Foulkes, *J. Appl. Electrochem.*, in preparation.
32. H.I. Philip, M.J. Nicol and A.M.E. Balaes, Rept. No. 1796, National Institute for Metallurgy, Johannesburg, South Africa (1976).
33. A. Saraby-Reintjes and M. Fleischmann, *Electrochim. Acta* **29** (1984) 557.